Available online at www.sciencedirect.com
ScienceDirect
Journal of Hazardous Materials 152 (2008) 1037–1044
Journal of Hazardous Materials
www.elsevier.com/locate/jhazmat

Photodegradation of an azo dye using immobilized nanoparticles of TiO_2 supported by natural porous mineral

Fangfei Li [a,b], Shenmei Sun [a,b], Yinshan Jiang [a,b,*], Maosheng Xia [a,b], Mengmeng Sun [a,b], Bing Xue [a,b]

[a] *Key Laboratory of Automobile Materials, Jilin University, Ministry of Education, Changchun 130026, PR China*
[b] *Department of Materials Science and Engineering, Jilin University, Changchun 130026, PR China*

Received 6 May 2007; received in revised form 24 July 2007; accepted 24 July 2007
Available online 7 August 2007

Abstract

Natural mordenite, replacing the synthetic zeolites, has been employed as the support of TiO_2, and its photocatalytic activity has been examined in methyl orange (MO) aqueous under UV light. AFM, TEM, XRD, FTIR and fluorescence spectra have been used to reveal the loading effects of TiO_2 on mordenite. The results show that the photocatalytic degradation (PCD) reaction rates are sharply increased by natural zeolite supports. Since mordenite is photo-inert, the PCD-enhancement is mostly caused by the bonding effects of Ti–O–Si and Ti–O–Al. Moreover, another two distinct natural zeolites have been employed as the supports of TiO_2, in order to check the universality of PCD-enhancement effect of natural zeolites on TiO_2. And the factors of PCD reaction on TiO_2–zeolite, such as pH and catalyst dose, have been investigated.

Keywords: Natural mordenite; Zeolite; Photocatalytic degradation; PCD-enhancement; TiO_2

1. Introduction

Nanoscaled TiO_2 particles have attracted a great deal of attentions in waste treatment, due to their high photocatalytic degradation (PCD) rate of various organic compounds [1–6]. But the recycling difficulties restricted the utilization of finer TiO_2 particles. Thus, in practical applications, TiO_2 nanoparticles have been considered to be fixed on inert and ideal supports [7–15]. Among various supporting materials, zeolites seem attractive candidates due to their unique uniform pores, super adsorption capability and special ion-exchangement ability [14–18]. Moreover, their inorganic framework keeps them from photo-decay.

As a typical porous material, zeolites can be divided into natural zeolites and synthetic zeolites. Natural zeolites are cheaper and more abundant, but have smaller channels as compared with synthetic zeolites. As a natural mineral resource, natural zeolites are easy to obtain and cause negligible chemical pollutions during the production process, but meet some difficulties in purification.

Previous works have simply emphasized on the synthetic zeolites as supports, and found that the employment of special species of synthetic zeolites benefit the photo-activity of loaded TiO_2 to some extent [14,19,20]. The reasons for such enhancement were explained variously, such as the adsorption ability [21], the preconcentration near the photoactive sites, the stability of intermediates (like hydroxyl radical), the delivery of organic substrates, and even the active structure of zeolite itself [14,22], etc. All of the origins indicate somewhat relationship with the porous structure, the adsorption capability and the ion-exchangement ability of zeolite supports, which are peculiar not only to the synthetic zeolites but also to the natural zeolites. That means natural zeolites are likely to be used as a potential substitute for the synthetic ones.

Considering the large-scale utilizations in practical, natural zeolites seems more ascendent than synthetic ones, due to their low cost, abundant and less chemical pollution during production. But, as we have known, comparing with the synthetic zeolites, natural zeolites have smaller channel size, and their species of structure are multiform. In view of these facts, whether

* Corresponding author at: Department of Materials Science and Engineering, Jilin University, No. 6 West-Minzhu Avenue, Changchun 130026, PR China.
E-mail addresses: jiangyinshan@163.com, yinshan_jiang@yahoo.com.cn (Y. Jiang).

0304-3894/$ – see front matter © 2007 Elsevier B.V. All rights reserved.
doi:10.1016/j.jhazmat.2007.07.114

the PCD-enhancement effect would be preserved after replacing synthetic zeolites with natural ones remains a question. However, studies on the natural zeolite supports are rare. It would be instructive to investigate the interaction between TiO_2 and natural zeolite supports in order to promote the practical applications of PCD on supported photoactive semiconductors for environmental purpose.

Based on the above point, in this article, the principal objective was to verify whether the PCD-enhancement effect could recur in the natural zeolite–TiO_2 system. A typical natural zeolite, mordenite, was employed as the support of nanoscaled TiO_2. And the kinetic process of PCD in methyl orange (MO) solution on different catalysts were monitored under UV irradiation. In addition, AFM, far FTIR, XRD and Fluorescence spectra were taken in order to reveal the interaction between natural zeolite and TiO_2. Moreover, another two widely used natural zeolites, laumontite and clinoptilolite, were also examined to check the universality of PCD-enhancement effect on natural zeolites.

2. Experimental

2.1. Synthesis

$Ti(OC_4H_9)_4$ (CR), ethanol (AR), HNO_3 (AR) were obtained from Beijing Chemical Co. All chemicals were used as received. Three types of natural zeolites were employed in this study. Natural mordenite was produced from Jiutai (Jilin province, PR China). Natural clinoptilolite was from Panshi (Jilin province, PR China). And natural laumontite was from Yangcaogou (Liaoning province, PR China). Some of their properties are listed in Table 1 [23]. The raw zeolites were grinded, purified, washed and then dried at 120 °C. All of the resultant raw natural zeolites were kept in desiccator until the synthesis of TiO_2–zeolite.

A transparent TiO_2 solution was prepared firstly. And the compound catalyst was synthesized by dropping a certain amount of TiO_2 solution onto the clean natural zeolite. The detailed preparation method for TiO_2–zeolite has been described previously [24–26]. The content of TiO_2 in natural zeolite was estimated to be 5 wt.%.

2.2. Photocatalytic experiments

The typical conditions of the PCD experiments are as follows: 0.04 g of TiO_2–zeolite (or 0.002 g pure TiO_2 powders) was put into 10 mL of MO aqueous solution, and was illuminated under high-Hg lamp of 250 W (Philips) having main wavelength 365 nm. The photocatalytic reactor configuration is shown in Scheme 1. The PCD reaction was monitored by UV-754 spectrophotometer at 463 nm-light [27]. The pH value of the reaction liquor was adjusted to 8. And the detailed experimental procedures have been described previously [24–26].

The PCD rate of MO was determined in two ways, k_1 and R_0, based on the absorbance data (A) collected by spectrophotometer during PCD reaction. A_0 was the initial absorbance value of MO solution at 463 nm. The pseudo-first-order rate constant (k_1) was calculated from the plotting of $\ln(A_0/A)$ versus t. The initial

Table 1
Structure properties of different natural zeolites [23]

Name	Molecular formula	Crystal form	Lattice constant (Å)	Dimension	Direction	Channel size (Å)	Pore volume (%)	Density of frame (g/cm^3)
Laumontite	$Ca_4[Al_8Si_{16}O_{48}]\cdot 16H_2O$	Oblique	$a = 14.90$, $b = 13.17$, $c = 7.50$, $\beta = 111°30'$	I	//a	4.6×6.3	34	1.77
Mordenite	$Na_8[Al_8Si_{40}O_{96}]\cdot 24H_2O$	Orthorhombic	$a = 18.13$, $b = 20.49$, $c = 7.52$	II	//c, //b	6.7×7.0; 2.9×5.7	28	1.70
Clinoptilolite[a]	$Na_8[Al_8Si_{40}O_{96}]\cdot 32H_2O$	Oblique	$a = 7.41$, $b = 17.89$, $c = 15.85$, $\beta = 91°29'$	II	//a, //c	4.0×5.5; 4.4×7.2, 4.1×4.7	34	1.71

[a] The "Direction" and "Channel Size" of clinoptilolite, which were not shown in Ref. [23], were extracted from the data of heulandite which has been considered to have similar structure to C.

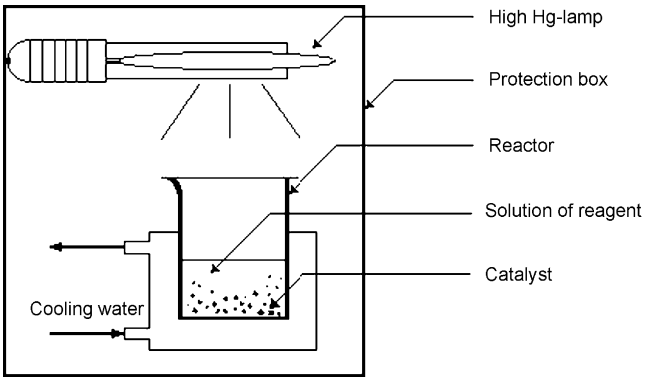

Scheme 1. Experimental photocatalytic reactor.

reaction rate (R_0) was expressed as

$$R_0 = \frac{dC}{dt} = \frac{C_0}{A_0}\frac{dA}{dt}$$

where C_0 is the initial concentration of MO. In order to get reliable data for R_0, the value of A was measured every 2 min at the initial stage of the PCD reaction. And the value of dA/dt was determined by the slope of the tangent line at experimental data points located on the curve of A versus t, i.e. the initial rate (R_0) was calculated from the tangent linear period.

Considering the slight degradation of MO under UV light, the PCD processes of pure MO and raw zeolites had been measured. During the calculation process of k_1 and R_0, mordenite were treated as the fundi of the PCD curves of TiO_2–mordenite, and the curves of MO were treated as the fundi of the PCD curves of pure TiO_2, respectively. Thus, the base degradation effects could be eliminated.

2.3. Characterization method

The structures of the samples were examined with an X-ray diffractometer (XRD; Shimadzu, D/max-rA with Cu Ka radiation). The morphology of the samples were obtained by atom force microscope (AFM; Dimension 3100, USA) and transmission electron microscope (TEM). And the bond vibration was analyzed by far Fourier transform infrared ray (far FTIR; Nexus 6700, USA) spectroscopy, which was carried out by polyethylene film and collected 70 scans at the range of 600–50 cm^{-1}. The fluorescence spectra were taken by He–Cd laser at λ_{ex} = 325 nm with resolution of 0.2 nm. Chemical oxygen demand (COD) was measured by the dichromate titration method.

3. Results and discussion

3.1. Characterization

Natural mordenite, whose structure was much approximate to the characteristics of synthetic zeolites, was employed as the support of TiO_2 in the beginning, due to its abundant reserve, large pore size and two-dimension channel network among various species of natural zeolites. And the XRD patterns are shown in Fig. 1. It should be noted that despite the raw zeolites had been purified before preparation, there still existed some inert impurities in the zeolites to some extent.

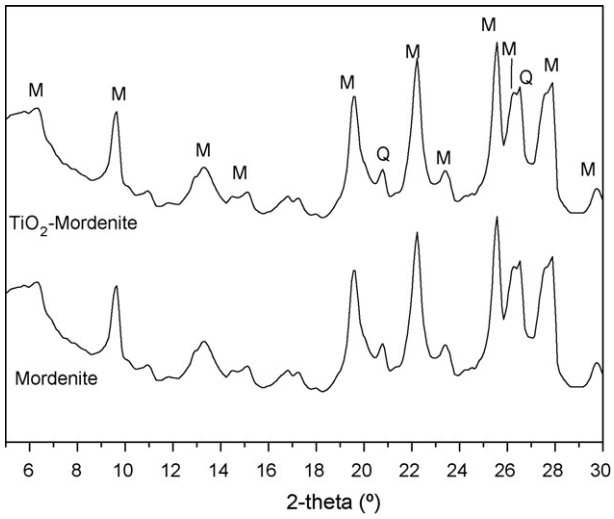

Fig. 1. XRD patterns of raw natural mordenite and TiO_2–mordenite: M and Q represent Mordenite and Quartz, respectively.

The mordenite materials before and after TiO_2 loading were characterized by AFM, TEM and XRD analysis. Fig. 2 shows the AFM phase images of mordenite and TiO_2–mordenite. It is obviously that the surface of mordenite is significantly changed after TiO_2 loading. The comparison between the two images indicates that the natural mordenite is covered with TiO_2 spheres of 50 nm or so. The loaded TiO_2 particles are in a non-dense-packing arrangement with some pores left.

Moreover, TEM image (Fig. 3) shows that the particle size of resultant pure TiO_2 nanopowders is around 80 nm, which is a little larger than the loaded TiO_2 on mordenite revealed by AFM analysis. This phenomenon consists with the previous results of other group [14]. It indicates that the colloid TiO_2 are no longer free particles at the presence of zeolites, and their crystal growth are restricted by the porous supports, leading to the observed decrease in the size of loaded TiO_2 particles.

Furthermore, XRD studies were undertaken to understand the crystalline structure of the mordenite before and after TiO_2 loading. According to Fig. 1, pattern of TiO_2–mordenite consists with the raw mordenite very well and there are no diffraction peaks corresponding to typical TiO_2, including anatase, rutile and brookite, can be observed. And similar results have also been reported by other researchers [17,28]. This should be due to the less amount and small-size of TiO_2 loaded on mordenite, which also corresponds to the morphology analysis. Particle size of TiO_2 loaded on zeolite is 50 nm (Fig. 2), which is the size of second sphere. That means the first sphere size must be much smaller than this, which might be below the detection sensitivity of the XRD technique (<40 Å) [29], resulting in the absence of the peaks of TiO_2 in the TiO_2–zeolite XRD pattern. The results also indicate that the frame structure of mordenite has been remained in the resultant compound photocatalyst.

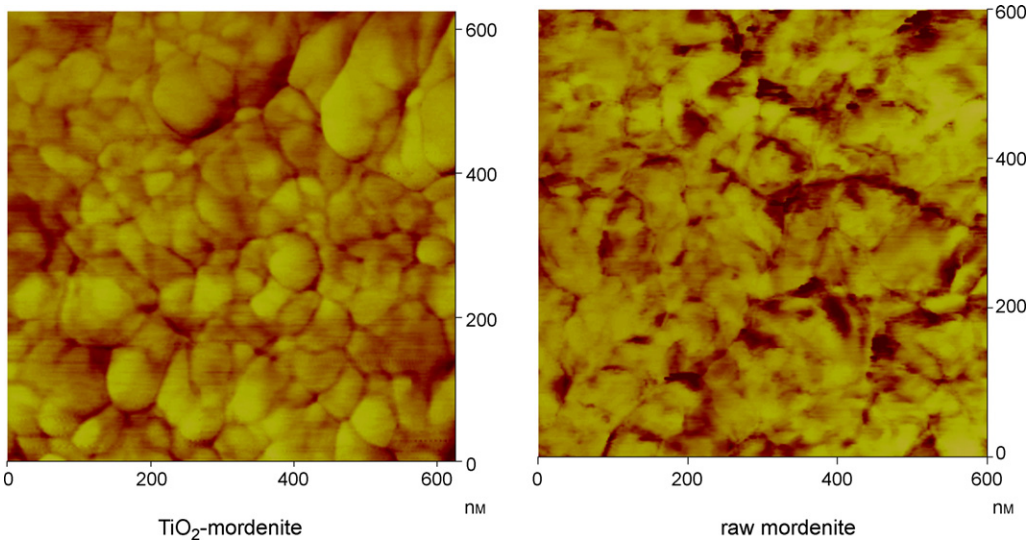

Fig. 2. AFM phase images of raw mordenite and TiO_2–mordenite.

3.2. Photocatalytic activities of TiO_2–mordenite and pure TiO_2

In this study methyl orange (MO) was chosen as model compound, which was considered to be one kind of recalcitrant azo dye. And the PCD processes of MO in aqueous heterogeneous system were measured under UV light, in order to determine the photocatalytic activities of different photocatalysts.

As the effect of pollutant concentration was important in any process of water treatment, PCD processes at various initial concentrations of MO (C_0) were investigated for the two photocatalysts. As shown in Fig. 4, all of the A–t curves follow linear principle at the initial stage, and match the pseudo-first-order discipline as a whole.

That means there are two reaction rates to describe the PCD process. The first is the initial reaction rate (R_0), which is determined by the slope of the tangent line at the initial stage of the experimental data points. The second is the pseudo-first-order reaction rate (k_1), which is calculated by a linear plot of $\ln(C_0/C) - t$. Both of the two reaction rates are summarized as a function of C_0 in Fig. 5 for different catalysts. It can be seen that the k_1 decreases with the initial concentration, which is quite common in PCD studies for many organic compounds in dilute solution [8,30]. And the value of R_0 of each catalyst fluctuates with C_0, which is approximate to a constant.

Taking the results of Fig. 5 into account, in both cases TiO_2–mordenite shows higher reaction rate than pure TiO_2 powder no matter how much the value of C_0 is, indicating that the photo-inert mordenite support has increased the photoactivity of TiO_2 significantly. That means, despite the impurities and smaller channels, natural mordenite also shows the PCD-enhancement effect which is similar to the synthetic zeolites. And this must be of grate moment for natural zeolites to replace the synthetic zeolites in large-scale utilizations of PCD treatment for environmental purpose.

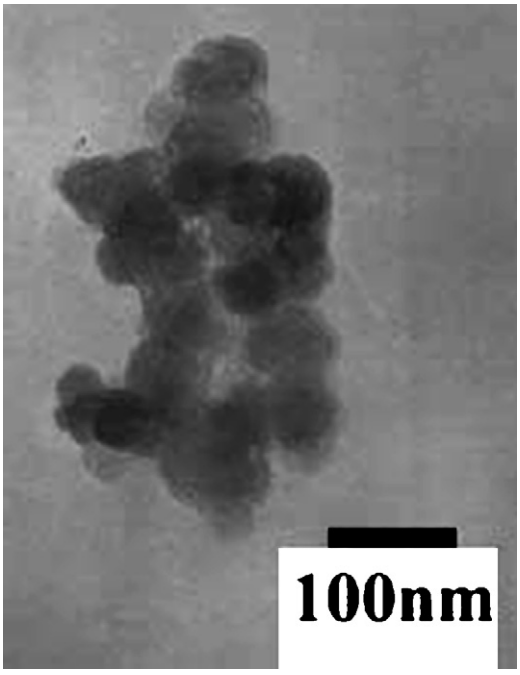

Fig. 3. TEM image of pure TiO_2 powders heated at 200 °C.

3.3. Interaction between natural mordenite and TiO_2

Mordenite is photo-inert, and do not participate in the PCD process forthrightly. In order to reveal the PCD-enhancement mechanism, further investigations were carried out by FTIR and fluorescence spectra to understand the loading effect between natural mordenite and TiO_2.

The combination or interface reaction effects were confirmed by far FTIR analysis. As shown in Fig. 6, the peak of compound catalyst shows red shift from 238 cm^{-1} (pure TiO_2) to 205 cm^{-1} (TiO_2–mordenite), which is considered to be the bonding effects of Ti–O–Si and Ti–O–Al [24].

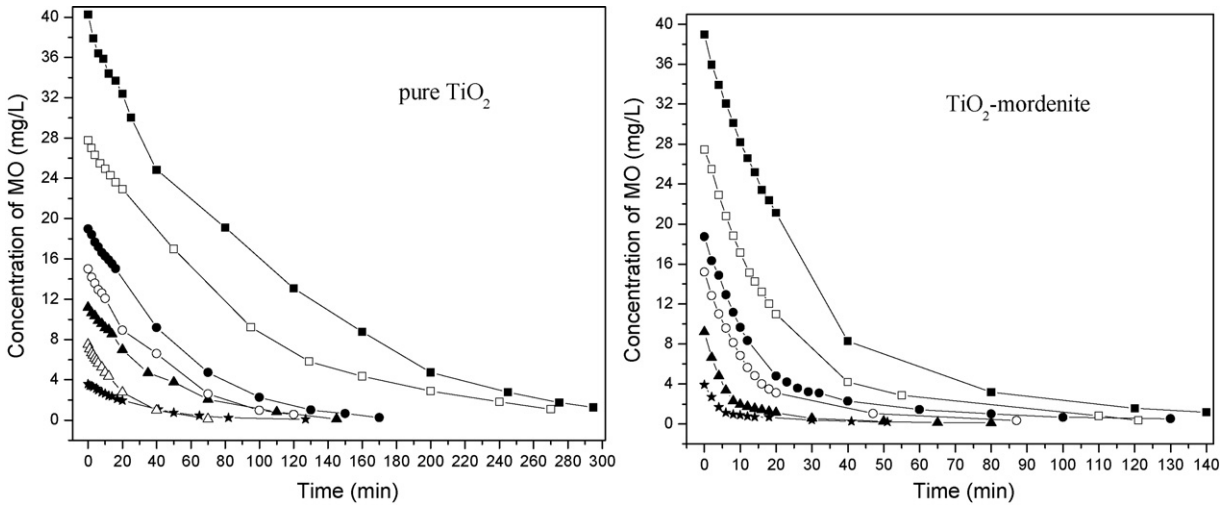

Fig. 4. PCD of MO as a function of illumination time for various initial concentrations (at the range of 4–40 mg/L) on TiO_2–mordenite and pure TiO_2.

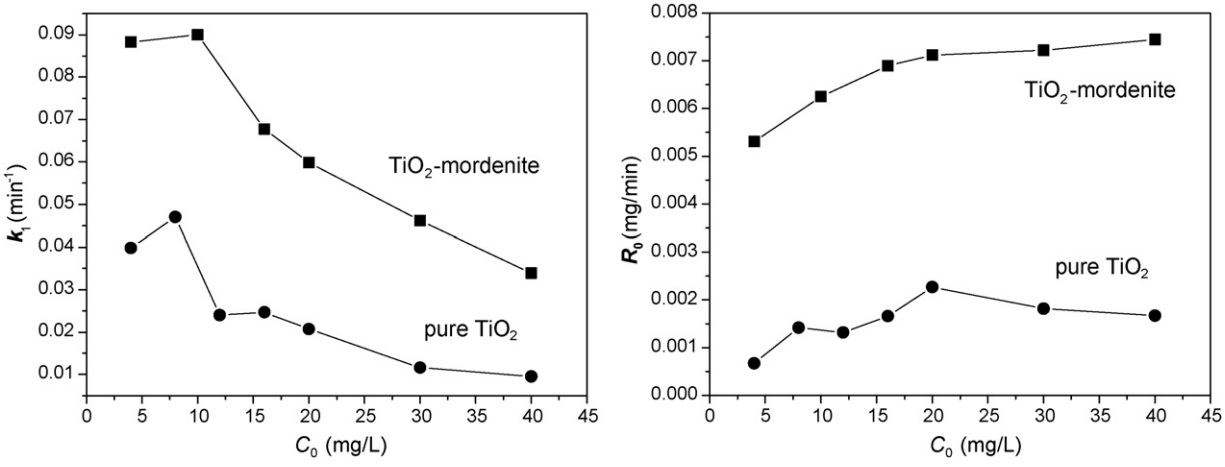

Fig. 5. k_1 and R_0 values of TiO_2 and TiO_2–mordenite at various initial concentration of MO (C_0 is at the range of 4–40 mg/L).

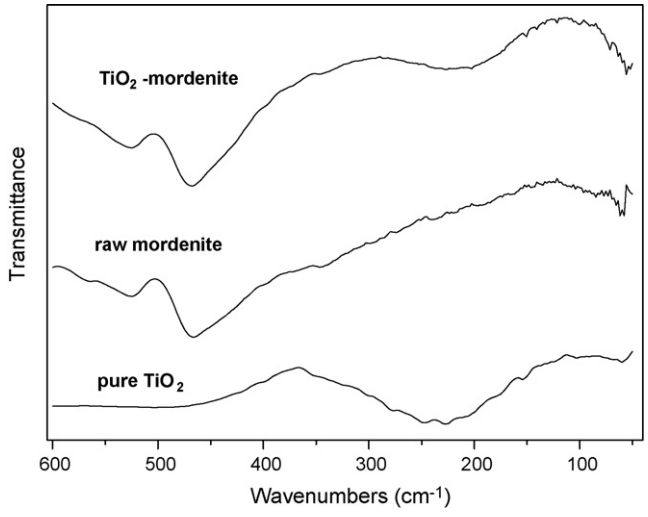

Fig. 6. Far FTIR spectra of pure TiO_2, raw mordenite and TiO_2–mordenite.

Furthermore, the fluorescence spectra ($\lambda_{ex} = 325$ nm) were taken. As shown in Fig. 7, the peak at 402 nm is the characteristic absorbing band of mordenite, which is caused by regular framework of porous silica, and its intensity is invariable. The peaks at the range of 475–600 nm reflect the existence of surface defects of natural mordenite. After TiO_2 loading, these peaks decay, indicating that a certain percentage of surface defects on raw mordenite combine with TiO_2 during the synthesis process and create new bonds such as Ti–O–Si and Ti–O–Al.

As has been discussed previously [24], the existence of the bondings of Ti–O–Si or Ti–O–Al may generate positive ion defects, which is considered to be the electron trapper at interface between mordenite and TiO_2, due to the combination of high positive ion (Ti^{IV}) with the surface O of mordenite. And this might be one of the origins for the PCD-enhancement effect.

3.4. Mineralization studies

Since the decrease in COD reflected the extent of mineralization of organic species, the COD removal percentage was measured to ascertain the complete degradation of MO. And the

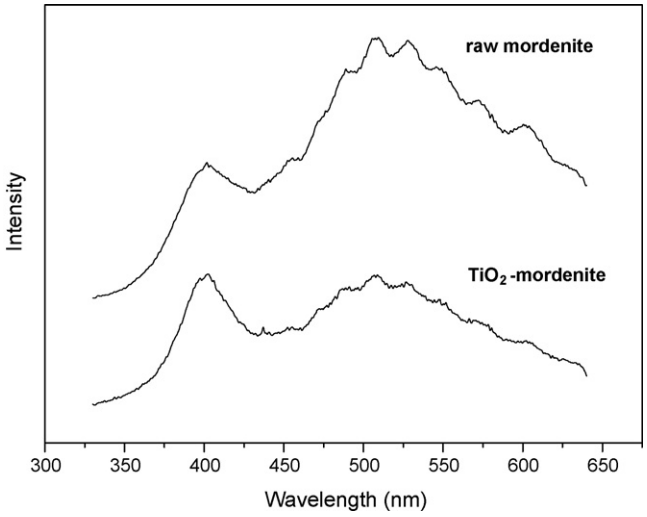

Fig. 7. Fluorescence spectra of mordenite before and after TiO_2 loading.

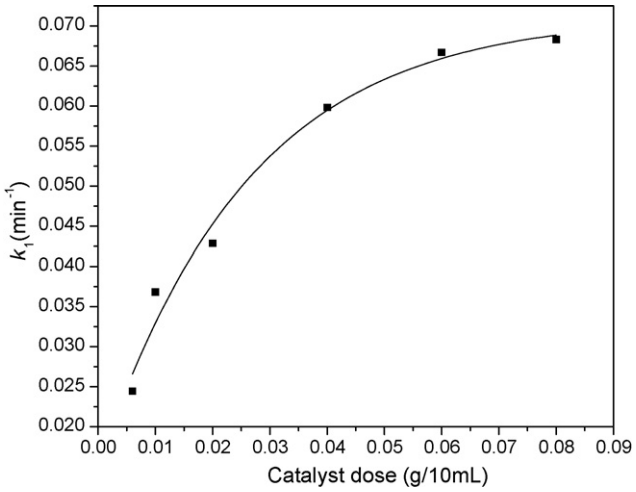

Fig. 9. PCD rate k_1 as a function of the dose of TiO_2–mordenite ($C_0 = 20$ mg/L, pH 8).

results are displayed in Fig. 8. As compared with the decolorization process, the COD removal process shows a little delay, due to the formation of smaller colorless intermediates during the PCD of MO. Furthermore, when the decolorization efficiency comes to 96.58% at the later period of PCD reaction (100 min), the corresponding COD removal percentage is 87.82%, indicating the overwhelming mineralization of MO. And considering the upward trend of the COD curve, longer irradiation is required in order to achieve the complete mineralization of dyes.

3.5. Effect of catalyst dose on PCD reaction

As the catalyst dose was one of the major kinetic factors of PCD reaction, a series of experiments were carried out by varying the amount of TiO_2–mordenite from 0.006 to 0.08 g/10 mL ($C_0 = 20$ mg/L, pH 8). The values of k_1 for various catalyst dose are depicted in Fig. 9. As seen, the PCD rate exhibits a sharp increase by increasing the catalyst dose from 0.006 to 0.04 g/10 mL, and the slop of the curve decreases with further increase in catalyst dose up to 0.08 g/10 mL, indicating that redundant catalyst shows little benefits in increasing the PCD rate.

3.6. Effect of initial pH on adsorption and PCD

As known, the value of pH makes great impressions on the conditions of medium, the surface charge distribution of TiO_2, and the adsorption behavior of absorbent. Therefore, the role of pH on the PCD and adsorption of MO on TiO_2–mordenite was studied at the pH range of 4–11 ($C_0 = 20$ mg/L, catalyst dose 0.04 g/10 mL). The pH of the solution was adjusted before irradiation and it was not controlled during the course of the reaction.

In the dark adsorption experiments, the TiO_2–mordenite was used only as absorbent, and the reactor was kept in dark for 4 h. The resulting decolorization efficiency of adsorption at various pH is shown in Fig. 10(a). The adsorption of dye on TiO_2–mordenite decreases with the value of pH, and approaches

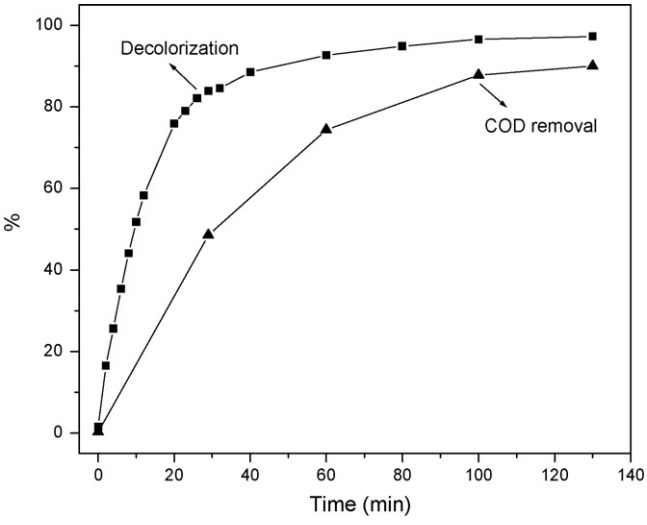

Fig. 8. The decolorization and mineralization process of MO on TiO_2–mordenite ($C_0 = 20$ mg/L, pH 8, catalyst dose 0.04 g/10 mL).

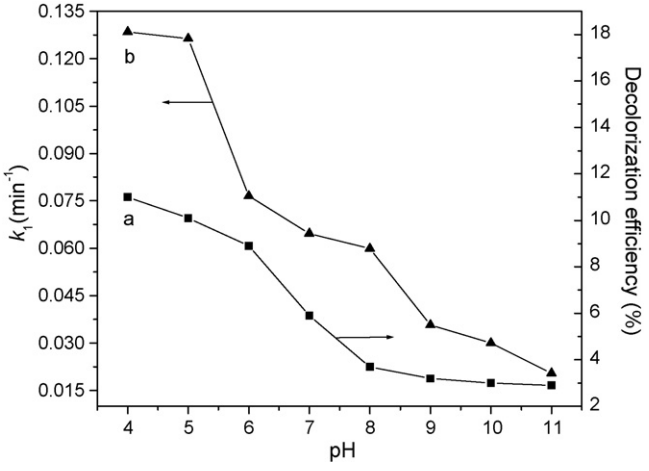

Fig. 10. Effects of initial pH on adsorption and PCD of MO on TiO_2–mordenite (a: dark adsorption for 4 h; b: k_1 of PCD).

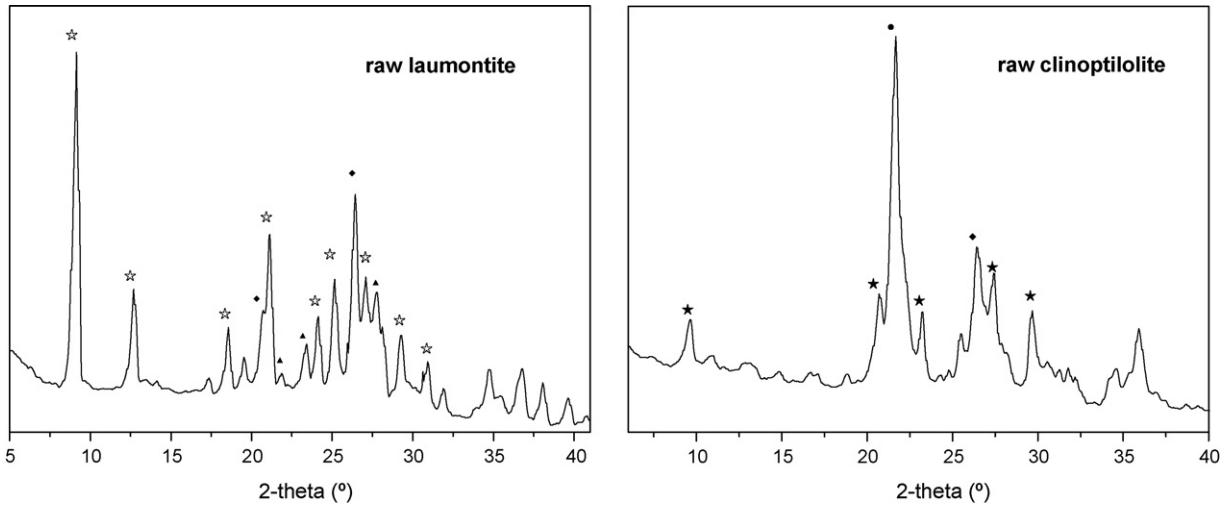

Fig. 11. XRD patterns of raw natural zeolites: (☆) laumontite; (⧫) quarts; (▲) feldspar; (⋆) clinoptilolite; (●) cristobalite.

a limit at 3% or so when the pH is more than 8. It might be caused by different chemical forms of MO at various pH. In strong acid conditions, MO is likely to change into quinine form, which is ionized and easy to be captured by zeolite absorbent. While in neutral and basic medium, MO is in azo form and only physical adsorption is taken place, resulting in the adsorption limit (3%).

As shown in Fig. 10(b), the pseudo-first-order rate (k_1) of PCD decreases sharply with pH value, and the value of k_1 keeps at low level in basic solution. As compared with dark adsorption process, both of the curves (a and b) decrease with pH, indicating somewhat relationship between the adsorption and photocatalytic activity of TiO_2–mordenite, although the basic of adsorption and degradation effects have been eliminated during the calculation process of k_1. Moreover, the highest adsorption decolorization efficiency is 11% (pH 4, 4 h), and the corresponding PCD reaction achieves 98% decolorization efficiency within 15 min. It means that in PCD process most of the decolorization of MO is caused by mineralization, which is also consists with the results of COD studies, and the adsorption of dye on catalyst only shows very slight effect on decolorization.

3.7. Effect of the species of natural zeolite on the PCD-enhancement effect

In order to examine the universality of PCD-enhancement effect on natural zeolites, another two distinct species of natural zeolites were employed as supports of TiO_2. Some of their properties are listed in Table 1 [23]. And their crystalline structure are shown in Fig. 11. Natural laumontite has the smallest pore size of the three and its pores are only in one-dimension. Clinoptilolite is a kind of natural zeolite in great reserve, whose pore size is a little smaller than mordenite. As the XRD pattern shows, the impurities in the raw clinoptilolite employed here are in great amount, which is quite common in natural zeolites due to the difficulties in purification. And this is constructive to derive whether the impurities show distinctly hazardous to the PCD-enhancement effect of natural zeolites.

The PCD processes at various C_0 of MO on TiO_2–clinoptilolite and TiO_2–laumontite were monitored. And their reaction rates are summarized in Fig. 12 (pH 8, catalyst dose 0.04 g/10 mL). It is obvious that the PCD rates

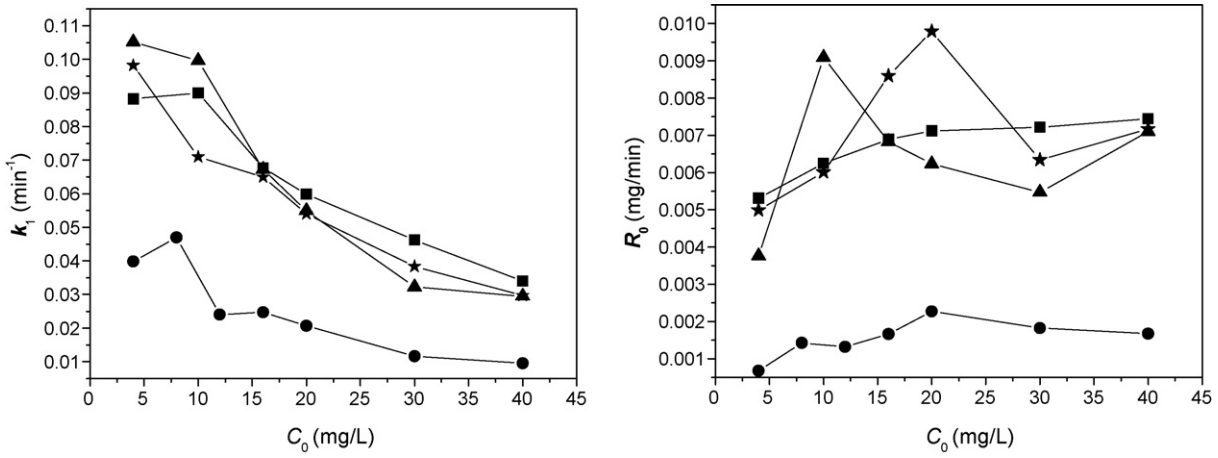

Fig. 12. k_1 and R_0 values of different catalysts at various initial concentration of MO (C_0): (●) TiO_2; (■) TiO_2–mordenite; (⋆) TiO_2–clinoptilolite; (▲) TiO_2–laumontite.

are sharply increased by natural zeolite supports, despite of the huge amount of the impurities in raw natural zeolites. The regularity of k_1 at various C_0 for these three TiO_2–zeolites are similar, all of which shows a downward trend with the increase of C_0. At the same time, in the case of R_0, the degree of the PCD-enhancement fluctuate slightly with the variety of natural zeolite species, which is caused by the different host structure and impurities. In a whole, the results suggest that PCD-enhancement effect is a universal phenomenon in natural zeolite-TiO_2 system, that means the feasibility of the substitution of natural zeolites for synthetic zeolites.

4. Conclusion

The comparative study of TiO_2 and TiO_2–zeolite has shown that natural zeolite supports benefit the PCD process of MO on TiO_2, indicating the feasibility of the substitution of natural zeolites for synthetic zeolites. Natural zeolites do not participate in the PCD process forthrightly, but they cause significant variations in morphology and combinations via interface reactions between zeolite surface defects and TiO_2 solution. The PCD process of TiO_2–mordenite is pH-dependent, and the reaction rate increases with the catalyst dose. COD studies show that the mineralization of MO is a little slower than the decolorization. Moreover, the species of natural zeolites and the existence of the impurities play a minor role in the PCD-enhancement effect of TiO_2.

Acknowledgements

The author gratefully thanks the financially supports of National Natural Science Foundation of China (Grant No. 40172020 and No. 50574043).

References

[1] D.F. Ollis, Contaminant degradation in water, Environ. Sci. Technol. 19 (1985) 480.
[2] M. Addamo, V. Augugliaro, A.D. Paola, E. García-López, V. Loddo, G. Marcì, R. Molinari, L. Palmisano, M. Schiavello, Preparation, characterization, and photoactivity of polycrystalline nanostructured TiO_2 catalysts, J. Phys. Chem. B 108 (2004) 3303.
[3] S.K. Kansal, M. Singh, D. Sud, Studies on photodegradation of two commercial dyes in aqueous phase using different photocatalysts, J. Hazard. Mater. 141 (2007) 581.
[4] M. Koelsch, S. Cassaignon, J.F. Guillemoles, J.P. Jolivet, Comparison of optical and electrochemical properties of anatase and brookite TiO_2 synthesized by the sol–gel method, Thin Solid Films 403/404 (2002) 312.
[5] N.M. Mahmoodi, M. Arami, N.Y. Limaee, N.S. Tabrizi, Kinetics of heterogeneous photocatalytic degradation of reactive dyes in an immobilized TiO_2 photocatalytic reactor, J. Colloid Interface Sci. 295 (2006) 159.
[6] N.M. Mahmoodi, N.Y. Limaee, M. Arami, S. Borhany, M. Mohammad-Taheri, Nanophotocatalysis using nanoparticles of titania mineralization and finite element modeling of solophenyl dye decolorization, J. Photochem. Photobiol. A: Chem. 189 (2007) 1.
[7] C. Lu, P. Yang, Y. Du, N. Hua, H. Song, Effects of supports on photocatalytic performance of supported TiO_2 catalysts, Chin. J. Catal. 24 (4) (2003) 248.
[8] A. Bouzaza, A. Laplanche, Photocatalytic degradation of toluene in the gas phase: comparative study of some TiO_2 supports, J. Photochem. Photobiol. A: Chem. 150 (2002) 207.
[9] K. Shimizu, T. Kaneko, T. Fujishima, T. Kodama, H. Yoshida, Y. Kitayama, Selective oxidation of liquid hydrocarbons over photoirradiated TiO_2 pillared clays, Appl. Catal. A: Gen. 225 (2002) 185.
[10] N.M. Mahmoodi, M. Arami, N.Y. Limaee, K. Gharanjig, Photocatalytic degradation of agricultural *N*-heterocyclic organic pollutants using immobilized nanoparticles of titania, J. Hazard. Mater. 145 (2007) 65.
[11] N.M. Mahmoodi, M. Arami, N.Y. Limaee, Photocatalytic degradation of triazinic ring-containing azo dye (Reactive Red 198) by using immobilized TiO_2 photoreactor: bench scale study, J. Hazard. Mater. B 133 (2006) 113.
[12] N.M. Mahmoodi, M. Arami, Bulk phase degradation of Acid Red 14 by nanophotocatalysis using immobilized titanium(IV) oxide nanoparticles, J. Photochem. Photobiol. A: Chem. 182 (2006) 60.
[13] C. Anderson, A.J. Bard, Improved photocatalytic activity and characterization of mixed TiO_2/SiO_2 and TiO_2/Al_2O_3 materials, J. Phys. Chem. B 101 (1997) 2611.
[14] Y. Xu, C.H. Langford, Photoactivity of titanium dioxide supported on MCM41, zeolite X, and zeolite Y, J. Phys. Chem. B 101 (1997) 3115.
[15] N. Takeda, T. Torimoto, S. Sampath, S. Kuwabata, H. Yoneyama, Effect of inert supports for titanium dioxide loading on enhancement of photodecomposition rate of gaseous propionaldehyde, J. Phys. Chem. 99 (1995) 9986.
[16] Z.Y. Ji, J.S. Yuan, X.G. Li, Removal of ammonium from wastewater using calcium form clinoptilolite, J. Hazard. Mater. 141 (2007) 483.
[17] Y. Kim, M. Yoon, TiO_2/Y-Zeolite encapsulating intramolecular charge transfer molecules: a new photocatalyst for photoreduction of methyl orange in aqueous medium, J. Mol. Catal. A: Chem. 168 (2001) 257.
[18] S. Anandan, M. Yoon, Photocatalytic activities of the nano-sized TiO_2-supported Y-zeolites, J. Photochem. Photobiol. C: Photochem. Res. 4 (2003) 5.
[19] N.P. Rhodes, R.J. Rudham, Catalytic studies with dealuminated Y zeolite. Part 2. Disproportionation of toluene, J. Chem. Soc., Faraday Trans. 90 (1994) 809.
[20] R.J. Rudham, A.W. Winstanley, Effects of dry-air calcination on the physico-chemical and catalytic properties of HZSM-5 zeolite, J. Chem. Soc., Faraday Trans. 90 (1994) 3191.
[21] C. Minero, F. Catozzo, E. Pelizzetti, Role of adsorption in photocatalyzed reactions of organic molecules in aqueous titania suspensions, Langmuir 8 (1992) 481.
[22] Y. Xu, C.H. Langford, Enhanced photoactivity of a titanium(IV) oxide supported on ZSM5 and zeolite A at low coverage, J. Phys. Chem. 99 (1995) 11501.
[23] D.W. Breck, Zeolite Molecular Sieves: Structure, Chemistry and Use, John Wiley and Sons, New York, 1974, p. 29.
[24] F. Li, Y. Jiang, L. Yu, Z. Yang, T. Hou, S. Sun, Surface effect of natural zeolite (clinoptilolite) on the photocatalytic activity of TiO_2, Appl. Surf. Sci. 252 (2005) 1410.
[25] S. Fang, Y. Jiang, A. Wang, Z. Yang, F. Li, Photocatalytic performance of natural zeolite modified by TiO_2, Chin. Non-Metallic Mines 27 (1) (2004) 14.
[26] S. Fang, Y. Jiang, Y. Wang, C. Bao, B. Song, Photocatalysis characterization of titanium dioxide supported on natural clinoplilolite, Chin. J. Environ. Sci. 24 (2003) 113.
[27] M.S. Masoud, H.H. Hammud, Electronic spectral parameters of the azo indicators: methyl red, methyl orange, PAN, and fast black K-salt, Spectrochim. Acta Part A 57 (2001) 977.
[28] H. Chen, A. Matsumoto, N. Nishimiya, K. Tsutsumi, Preparation and characterization of TiO_2 incorporated Y-zeolite, Colloids Surf. A: Physicochem. Eng. Aspects 157 (1999) 295.
[29] M. Cozzolino, M. Di Serio, R. Tesser, E. Santacesaria, Grafting of titanium alkoxides on high-surface SiO_2 support: an advanced technique for the preparation of nanostructured TiO_2/SiO_2 catalysts, Appl. Catal. A: Gen. 325 (2007) 256.
[30] Y. Xu, C.H. Langford, Variation of langmuir adsorption constant determined for TiO_2-photocatalyzed degradation of acetophenone under different light intensity, J. Photochem. Photobiol. A: Chem. 133 (2000) 67.